Published in final edited form as:
Nano Lett. 2010 August 11; 10(8): 2843–2848. doi:10.1021/nl1008635.

In Vitro and *In Vivo* Studies of Single-Walled Carbon Nanohorns with Encapsulated Metallofullerenes and Exohedrally Functionalized Quantum Dots

Jianfei Zhang[†], **Jiechao Ge**[†], **Michael D. Shultz**[≠], **Eunna Chung**[‡], **Gurpreet Singh**[ζ], **Chunying Shu**[†], **Paul A. Deck**[†], **Panos P. Fatouros**[≠], **Scott C. Henderson**[#], **Frank D. Corwin**[≠], **David B. Geohegan**[§], **Alex A. Puretzky**[§], **Christopher M. Rouleau**[§], **Karren More**[§], **Christopher Rylander**[‡], **Marissa Nichole Rylander**[‡], **Harry W. Gibson**[†], and **Harry C. Dorn**[†,*]

[†]Department of Chemistry, Virginia Polytechnic Institute and State University, Blacksburg, VA 24060

[‡]Department of Mechanical Engineering and School of Biomedical Engineering and Sciences, Virginia Polytechnic Institute and State University, Blacksburg, VA 24060

[ζ]Institute for Critical Technology and Applied Science, Virginia Polytechnic Institute and State University, Blacksburg, VA 24060

[≠]Department of Radiology, Virginia Commonwealth University, Richmond, VA, 23298

[#]Department of Anatomy & Neurobiology, Virginia Commonwealth University, Richmond, VA, 23298

[§]Center for Nanophase Materials Sciences and SHARE Facilities, Oak Ridge National Laboratories, Oak Ridge, TN, 37831

Abstract

Single-walled carbon nanohorns (SWNHs) are new carbonaceous materials. In this paper, we report the first successful preparation of SWNHs encapsulating trimetallic nitride template endohedral metallofullerenes (TNT-EMFs). The resultant materials were functionalized by a high-speed vibration milling method and conjugated with CdSe/ZnS quantum dots (QDs). The successful encapsulation of TNT-EMFs and external functionalization with QDs provide a dual diagnostic platform for *in vitro* and *in vivo* biomedical applications of these new carbonaceous materials.

Keywords

Carbon nanohorns; peapods; quantum dots; *in vitro*; *in vivo*

Carbon nanomaterials, such as fullerenes and nanotubes, have been studied for decades for their unique properties and various applications. In 1999, Iijima's group reported a new type of carbon nanomaterial, single-walled carbon nanohorns (SWNHs). SWNHs are closed tubules, typically 2-10 nm in diameter and 10-70 nm long, which are composed of single graphitic layers terminating with conical ends.1, 2 During synthesis, SWNHs form aggregates 40~200 nm in diameter. The size of the aggregates depends on the length of individual SWNHs and can be adjusted by limiting the growth time with an adjustable

[*]**Correspondence author:** Harry C. Dorn, Department of Chemistry, Virginia Polytechnic Institute and State University, Blacksburg, VA, 24060; hdorn@vt.edu; Phone: 540-231-5953; Fax: 540-231-3255.

pulse-width laser.3 SWNHs have significant advantages over traditional carbon nanotubes for *in vivo* biotechnology because no metal catalyst is used in the production, and their aggregates are naturally within the size range of endocytosis. Recent research reports also indicate that SWNHs have low toxicity.4, 5 These features make SWNHs uniquely suited for various medical applications, such as laser therapeutic agents,6, 7 antiviral materials,8 anticancer agents,9, 10 etc. By encapsulating other species, SWNHs can also be used as drug delivery systems10-17 and magnetic resonance imaging (MRI) contrast agents.18, 19 However, these medical applications are limited by the hydrophobic nature of the SWNHs. Many efforts have been made to disperse SWNHs in aqueous solution, both by covalent functionalization and noncovalent modification.14, 15, 20-26 Recently, we developed a facile high speed vibration milling (HSVM) method to prepare water-dispersible SWNHs functionalized with carboxyl groups.27 The carboxylated carbon materials can be further conjugated with other materials, such as quantum dots (QDs).28-30 QDs are semiconducting nanocrystals for which the electronic and optical properties can be tuned by altering the size due to the quantum confinement effect.31 The SWNH-QDs conjugate can be used for multiple functions such as bio-sensing.

In this report, we show the first successful encapsulation of trimetallic nitride template endohedral metallofullerenes (TNT-EMFs) inside SWNHs (SWNH peapods). Two kinds of TNT-EMFs were used for the encapsulation: $Gd_3N@C_{80}$ and $Lu_3N@C_{80}$. $Gd_3N@C_{80}$ can be used as MRI contrast agents, while $Lu_3N@C_{80}$ can be used as X-ray contrast agent32 and radiotherapeutic agents33 if ^{177}Lu is used. The SWNH peapods were functionalized by the HSVM method and further conjugated with ZnS-capped CdSe (CdSe/ZnS) QDs. The materials were studied both *in vitro* and *in vivo*.

In our research, SWNHs (estimated carbon purity ≥95%) were synthesized by Nd:YAG laser (λ=1.064 μm, 20 ms pulse width) vaporization of a carbon target into an argon atmosphere at 1100°C. TNT-EMFs, $Gd_3N@C_{80}$ and $Lu_3N@C_{80}$, were produced and purified as previously reported.34, 35 Succinic acid acyl peroxide was synthesized according to the literature.36 CdSe/ZnS QDs (Emission: 577 nm, FWHM < 24 nm) were purchased from Ocean Nano Tech LLC.

The SWNH peapods were prepared by heating SWNHs at 650 °C in air for 10 minutes to remove amorphous carbon and open windows on the tips and walls. After cooling, TNT-EMFs were dissolved in CS_2 and dropped onto the SWNHs. The solvent was evaporated. The mixture of fullerenes and SWNHs was sealed in a quartz tube under 10^{-6} Torr. The tube was heated at 470°C for 24 hours. The product was sonicated in toluene for 10 minutes. The solution was filtered through a 0.45 μm polytetrafluoroethylene (PTFE) membrane filter. The solid was washed with toluene until the extract was clear. The TEM samples were prepared by dispersing SWNH peapods in 1, 2-dichloroethane and dropped onto lacey carbon TEM grids.

HRTEM images of $Lu_3N@C_{80}$@SWNHs are shown in Figure 1. In the bright field image (Figure 1a) at lower magnification fullerene molecules appear to be small circles inside SWNHs. The high angle angular dark field (HAADF) image at higher magnification comfirmed the peapod structue. Due to the significant Z-contrast of HAADF, the Lu atoms appear to be bright spots inside SWNHs (grey area). When the fullerene molecule was at the right orientation, the Lu_3N cluster appears to be an equilateral triangle as the white circle shows. Similar results were also obtained for $Gd_3N@C_{80}$@SWNHs. (See supporting information)

SWNH peapods were functionalized by the HSVM method.27 The SWNH peapods were mixed with succinic acid acyl peroxide (mass ratio of SWNH peapods:peroxide=1:100). The

mixture was put into a stainless steel capsule and shaken vigorously for 2 hours (SPEX 8000 Mixer/Mill, 1725 rpm). The product was treated with acetone and centrifuged. The supernatant was decanted. The washing procedure was repeated three times to remove excessive succinic acid acyl peroxide. The final solid product was washed with water twice and sonicated in pure water for 20 minutes. A dark homogeneous suspension was obtained that was stable for several months.

CdSe/ZnS QDs were conjugated with $Gd_3N@C_{80}$@SWNHs. The method was similar to a published procedure as depicted in Scheme 1.28 Prior to conjugation of $Gd_3N@C_{80}$@SWNHs with QDs, the QDs surfaces were functionalized with amino groups. Briefly, QDs were suspended in chloroform via sonication for 30 min. Aqueous 1.0 M 2-aminoethanethiol hydrochloride (AET) was added to the QDs solution. Two layers were formed: the organic layer of chloroform-QDs suspension and the aqueous layer with AET. The mixture was stirred vigorously over night and allowed to settle for a few minutes. An equal volume of phosphate buffered saline solution (PBS) was then added and the mixture was stirred over night. The QDs were all transferred into the aqueous phase, which was collected and centrifuged. The precipitated QDs were then resuspended in PBS. To fabricate the $Gd_3N@C_{80}$@SWNH-QDs complexes, 1 mg of functionalized $Gd_3N@C_{80}$@SWNHs was suspended in 4 mL of PBS by sonication. N-(3-Dimethylaminopropyl)-N'ethylcarbodiimide hydrochloride (EDC, 115mg) and *N*-hydroxysulfosuccinimide (Sulfo-NHS, 2.8 mg) were added and the mixture was stirred for 5 min. Then 2 mL of functionalized QDs (2 mg/mL) in PBS were added and the resulting solution was stirred at 50 °C for 20 hours. The $Gd_3N@C_{80}$@SWNH-QDs suspension was filtered through a 0.2 μm Nylon membrane. The solid was washed with pure water. In control experiments for both functionalized SWNH peapods and the SWNH peapods conjugated with QDs, we have found no evidence for diffusion of the TNT-EMFs out of the SWNHs. (See Supplement Information).

Since the encapsulated TNT-EMFs contain paramagnetic Gd^{3+} ions, they substantially increase the ^1H relaxation rates of water (or biological system) and are potentially a new MRI contrast agent platform. The effect of these materials as potential MRI contrast agents was studied both *in vitro* and *in vivo*. The MRI experiments were performed on a 2.4 T/40 cm bore MR system (Biospec/Bruker). Tubes of different functionalized $Gd_3N@C_{80}$@SWNHs materials were imaged in a phantom well to obtain T_1-weighted (T_1W) images (T_R/T_E 700/10 ms), T_2-weighted (T_2W) images (T_R/T_E 6000/100 ms), and T_1-maps. The latter represents pure T_1 maps that are generated from a series of T_1W images. The Gd concentration of the samples was determined by inductively coupled plasma-mass spectrometry (ICP-MS) measurements. Samples were prepared for ICP-MS in glass vials that were washed in 10% trace metal grade nitric acid for 48 hours prior to sample addition. Optima grade nitric acid and heating to ~100°C was utilized to digestively prepare the samples, followed by dilution to a known volume with 18.2 MΩ deionized water.

Figure 2 shows the T_1-weighted, T_2-weighted and T_1 maps images of various SWNHs based materials, our previously reported *in vitro* $Gd_3N@C_{80}(OH)_{\sim 26}(CH_2CH_2COOM)_{\sim 16}$37 and the commercial Omniscan agent at similar concentrations. The empty functionalized SWNHs (Figure 2A) shows no enhancement while the $Gd_3N@C_{80}(OH)_{\sim 26}(CH_2CH_2COOM)_{\sim 16}$ (Figure 2D) provides the highest contrast. The functionalized $Gd_3N@C_{80}$@SWNHs (Figure 2B) exhibited reduced contrast compared to $Gd_3N@C_{80}(OH)_{\sim 26}(CH_2CH_2COOM)_{\sim 16}$ (Figure 2D), but the contrast is still significant for visualization. The reason for the reduced enhancement with the encapsulated fullerenes can be explained by the significant water exchange barrier between the encapsulated Gd^{3+} ions and bulk water molecules due to the additional graphitic layer of the SWNHs. This effective

distance was increased further when QDs were conjugated (Figure 2C) to the surface of SWNHs, and thus led to even lower contrast enhancement.

To determine the ability of $Gd_3N@C_{80}$@SWNH-QDs to label cancer cells for diagnosis or permit intracellular uptake for potential drug delivery applications, *in vitro* cell cultures were imaged using QDs fluorescence. A murine renal cancer cell line, RENCA, (CRL-2947, American Type Culture Collection) was cultured in RPMI 1640 media with L-glutamine (Mediatech) and supplemented with 10% fetal bovine serum, 1% Pen-Strep (Sigma-Aldrich), and 1% sodium pyruvate (Mediatech). Cells were seeded at a density of 1.5×10^4/well in 8-well Lab-Tek™ II CC2 chamber slide systems (Nunc, Rochester, NY). Cells were allowed to adhere for 24 hours. $Gd_3N@C_{80}$@SWNH-QDs were added to the media to obtain a concentration of 0.025 mg/ml and introduced to cells for incubation durations of 24 and 48 hours. Fluorescence and phase contrast images of RENCA cells were acquired before and following the 24 and 48 hours incubation with $Gd_3N@C_{80}$@SWNH-QDs using a Leica fluorescence inverted microscope (CTR6500, Leica Microsystems Inc., Bannockburn, IL) with a 20X objective. Cells without $Gd_3N@C_{80}$@SWNHs-QDs inclusion served as the control group. Figure 3 shows phase contrast and fluorescence images of RENCA cells without $Gd_3N@C_{80}$@SWNH-QDs inclusion (A,B) and following incubation for 24 hrs with $Gd_3N@C_{80}$@SWNH-QDs (D,E). Figures 3C and F show fluorescent images of the previously mentioned samples superimposed on phase contrast images to permit enhanced visualization of the correlation between cellular structure and quantum dots fluorescence. Negligible fluorescence signal was detected in the sample without $Gd_3N@C_{80}$@SWNH-QDs. The fluorescence shown in the bottom of Figure 3C is associated with autofluorescence of debris. However, inclusion of $Gd_3N@C_{80}$@SWNH-QDs for 24 hours and 48 hours (not shown) showed substantial and nearly identical levels of red fluorescence allowing imaging of the RENCA cells. The red fluorescence is entirely confined to the cell cytoplasm without any quantum dots visible in the extracellular media, providing evidence of cellular uptake. Due to the small size of the $Gd_3N@C_{80}$@SWNH-QDs, it is anticipated that significant cellular uptake occurs rapidly within minutes of $Gd_3N@C_{80}$@SWNH-QDs introduction. However, future experiments measuring cellular uptake kinetics are required to confirm this hypothesis. Therefore, inclusion of $Gd_3N@C_{80}$@SWNH-QDs provide significant contrast enhancement based on their fluorescence signature necessary for imaging of RENCA cells and exhibit substantial levels of cellular uptake critical for clinical applications involving drug delivery.

The *in vivo* investigation was performed by intratumoral infusion of $Gd_3N@C_{80}$@SWNH-QDs via convection enhanced delivery (CED) method into a U87 tumor bearing mouse. All experiments involving the use of mice were done in accordance with protocols approved by our Animal Care and Use Committee. Female athymic Nu/Nu mice 6-8 weeks old were anesthetized with I.P. ketamine/xylazine (70-140/14-28 mg/kg) and placed in a stereotactic frame (David Kopf Instruments). An incision site on top of the head was disinfected with betadine and alcohol. After a midline incision, a 0.7 mm burr hole was drilled in the skull located 0.5 mm anterior to the bregma and 2 mm laterally to the right. A 25 μL Hamilton Syringe with a 28 G removable needle was used to inject 1×10^5 U87 cells in 2 μL of PBS at a depth of 4.0 mm from the surface of the skull. Following the procedure, the animals were allowed to recover and then placed in the vivarium. The tumors were monitored by MRI scans with tail vein injections of OMNISCAN™ every 2-3 days starting 7 days post tumor implantation. On day 11 post tumor implantation, the $Gd_3N@C_{80}$@SWNH-QDs were infused into the developed intracerebral tumor by CED using a micro-injection pump (Bioanalytical Systems) at a flow rate of 0.2 μL/min for a total of 18 μL injected. The animals were scanned by MRI for baseline data immediately prior to intra-tumor infusion, and at time points of 0, 24, and up to 72 hours post infusion. Animals were then euthanized by ketamine/xylazine (280/56 mg/kg i.p.) and transcardially perfused with saline followed

by 4% paraformaldehyde in PBS. Whole brains were extracted and further fixed in 4% paraformaldehyde overnight. Coronal sections (50 μm) were cut on a VT1000S vibratome (Leica Microsystems) and stored in PBS.

The sections were washed 3 times (30 minutes each) in PBS, stained with 4′,6-diamino-2-phenylindole (DAPI, 0.1 μg/mL) for 10 minutes, and washed 3 additional times (10 minutes each) in PBS. The sections were mounted in Vectashield (Vector Laboratories) under #1.5 coverslips and sealed with nail varnish. Confocal microscopic images were collected using a Leica TCS-SP2 AOBS confocal laser scanning microscope (inverted) equipped with a spectrophotometer scan head, a Märzhäuser MCX-2 motorized XY stage and three photomultiplier tube detectors (PMT). Images were collected using a 20x/0.7 NA HC PlanApo multi-immersion objective lens, a scan resolution of 1024 × 1024 pixels and a zoom factor of 1. This gave a field size of 750 μm × 750 μm. Fluorescence from DAPI and CdSe/ZnS QDs was generated by exciting the samples with a blue diode laser (405 nm). Due to the significant degree of broad spectrum autofluorescence within the tumor, the signal from the quantum dots was isolated from that of the overlying autofluorescence by collecting a lambda series of images across the spectrum and subsequently unmixing the signals using the Spectral Dye Separation module of the Leica confocal software (LCS ver. 2.5.1347a). A series of 30 images (bit depth = 12) was collected over a range of 300 nm (410 – 710 nm) using a detector window of 20 nm. Post-acquisition, the signals of DAPI, QD and autofluorescence were isolated using standard reference spectra for DAPI and Quantum Dots (Em. peak: 577 nm, FWHM 24 nm) and the collected spectrum for the tissue autofluorescence.

The *in vivo* data shown in Figure 4 clearly illustrate the brightening of the T_1-weighted MRI image in the region of infusion due to the contrast enhancement by the $Gd_3N@C_{80}$@SWNH-QDs. Figure 4A is a T_1W image of the tumor enhanced by OMNISCAN™ (tail vein injection) 10 days post tumor cell inoculation. Figure 4B is the baseline T_1W image obtained day 11 just prior to intratumoral infusion of the $Gd_3N@C_{80}$@SWNH-QDs, while Figure 4C was collected 3 hours post infusion showing bright contrast at the infusion site within the tumor. The $Gd_3N@C_{80}$@SWNH-QDs were tracked by MRI 1 day post infusion (Figure 4D) and 3 days post (Figure 4E) which demonstrates that the SWNHs have a significant lifetime within the tumor, remaining long enough for potential local drug delivery, therapy, and long-term diagnosis. Also, if radioactive $^{177}Lu_3N@C_{80}$ were co-encapsulated inside SWNHs, the materials can be used as a dual modality for diagnosis and brachytherapy. Figure 4F is a high magnification composite confocal laser scanning microscope image of a region from a coronal section of the mouse brain (white square figure 4E) obtained following euthanization of the animal (3 days post infusion). The red fluorescent signal of the QDs is seen within the bright contrast area on the MR image Figure 4E (black arrow) which gives indication that the QDs remain bound to the SWNHs. This conjugation scheme can lead to further therapeutic agents remaining bound to the SWNHs or with further ratio optimization, the QDs can be used as another tracking mode to investigate bio-distribution of the material by fluorescence imaging.

In conclusion, TNT-EMFs, $A_3N@C_{80}$ (A=Gd and Lu), were encapsulated into SWNHs for the first time. The SWNH peapods were functionalized with carboxyl groups by an HSVM method and conjugated with CdSe/ZnS QDs. *In vitro* and *in vivo* experiments demonstrate the potential of the SWNHs-based materials as multi-modal diagnostic MRI contrast agents.

Supplementary Material

Refer to Web version on PubMed Central for supplementary material.

Acknowledgments

This work was partially funded by the National Institute of Health Grants 1 R21 CA135230-01 and CA119371. User research at the Center for Nanophase Materials Sciences and SHaRE Facility at ORNL sponsored by the Department of Energy, BES-DSUF. Nanohorn synthesis science funded by Department of Energy, BES-DMSE. Confocal microscopy was performed at the VCU - Department of Neurobiology & Anatomy Microscopy Facility, supported, in part, with funding from NIH-NINDS Center core grant 5P30NS047463.

References

1. Iijima S, Yudasaka M, Yamada R, Bandow S, Suenaga K, Kokai F, Takahashi K. Chem. Phys. Lett. 1999; 309(3,4):165–170.
2. Zhang M, Yamaguchi T, Iijima S, Yudasaka M. J. Phys. Chem. C. 2009; 113(26):11184–11186.
3. Puretzky AA, Styers-Barnett DJ, Rouleau CM, Hu H, Zhao B, Ivanov IN, Geohegan DB. Appl. Phys. A: Mater. Sci. Process. 2008; 93(4):849–855.
4. Miyawaki J, Yudasaka M, Azami T, Kubo Y, Iijima S. ACS Nano. 2008; 2(2):213–226. [PubMed: 19206621]
5. Lynch RM, Voy BH, Glass DF, Mahurin SM, Zhao B, Hu H, Saxton AM, Donnell RL, Cheng M-D. Nanotoxicology. 2007; 1(2):157–166.
6. Zhang M, Murakami T, Ajima K, Tsuchida K, Sandanayaka Atula SD, Ito O, Iijima S, Yudasaka M. Proc. Nat. Acad. Sci. USA. 2008; 105(39):14773–8. [PubMed: 18815374]
7. Miyako E, Nagata H, Hirano K, Makita Y, Nakayama K.-i. Hirotsu T. Nanotechnology. 2007; 18(47):475103/1–475103/7.
8. Miyako E, Nagata H, Hirano K, Sakamoto K, Makita Y, Nakayama K.-i. Hirotsu T. Nanotechnology. 2008; 19(7):075106/1–075106/6.
9. Ajima K, Murakami T, Mizoguchi Y, Tsuchida K, Ichihashi T, Iijima S, Yudasaka M. ACS Nano. 2008; 2(10):2057–2064. [PubMed: 19206452]
10. Ajima K, Yudasaka M, Murakami T, Maigne A, Shiba K, Ijima S. Mol. Pharm. 2005; 2(6):475–480. [PubMed: 16323954]
11. Murakami T, Ajima K, Miyawaki J, Yudasaka M, Iijima S, Shiba K. Mol. Pharm. 2004; 1(6):399–405. [PubMed: 16028351]
12. Xu JX, Yudasaka M, Kouraba S, Sekido M, Yamamoto Y, Iijima S. Chem. Phys. Lett. 2008; 461(4-6):189–192.
13. Venkatesan N, Yoshimitsu J, Ito Y, Shibata N, Takada K. Biomaterials. 2005; 26(34):7154–7163. [PubMed: 15967493]
14. Matsumura S, Ajima K, Yudasaka M, Iijima S, Shiba K. Mol. Pharm. 2007; 4(5):723–729. [PubMed: 17685580]
15. Murakami T, Sawada H, Tamura G, Yudasaka M, Iijima S, Tsucbida K. Nanomedicine. 2008; 3(4):453–463. [PubMed: 18694307]
16. Utsumi S, Urita K, Kanoh H, Yudasaka M, Suenaga K, Iijima S, Kaneko KJ. Phys. Chem. B. 2006; 110(14):7165–7170.
17. Yudasaka M, Murakami T, Ajima K, Miyawaki J, Shiba K, Iijima S. Pharm Tech Jpn. 2005; 21(12):2108–2112. Rinji Zokang.
18. Miyawaki J, Yudasaka M, Imai H, Yorimitsu H, Isobe H, Nakamura E, Iijima S. Adv. Mater. (Weinheim, Ger.). 2006; 18(8):1010–1014.
19. Miyawaki J, Yudasaka M, Imai H, Yorimitsu H, Isobe H, Nakamura E, Iijima S. J. Phys. Chem. B. 2006; 110(11):5179–5181. [PubMed: 16539444]
20. Rubio N, Herrero MA, Meneghetti M, Diaz-Ortiz A, Schiavon M, Prato M, Vazquez E. J. Mater. Chem. 2009; 19(25):4407–4413.
21. Pagona G, Karousis N, Tagmatarchis N. Carbon. 2008; 46(4):604–610.
22. Mountrichas G, Ichihashi T, Pispas S, Yudasaka M, Iijima S, Tagmatarchis N. J. Phys. Chem. C. 2009; 113(14):5444–5449.
23. Pagona G, Rotas G, Petsalakis ID, Theodorakopoulos G, Fan J, Maigne A, Yudasaka M, Iijima S, Tagmatarchis N. J. Nanosci. Nanotechnol. 2007; 7(10):3468–3472. [PubMed: 18330159]

24. Pagona G, Fan J, Maigne A, Yudasaka M, Iijima S, Tagmatarchis N. Diamond Relat. Mater. 2007; 16(4-7):1150–1153.
25. Tagmatarchis N, Maigne A, Yudasaka M, Iijima S. Small. 2006; 2(4):490–494. [PubMed: 17193072]
26. Murakami T, Fan J, Yudasaka M, Iijima S, Shiba K. Mol. Pharm. 2006; 3(4):407–414. [PubMed: 16889434]
27. Shu C, Zhang J, Ge J, Sim JH, Burke BG, Williams KA, Rylander NM, Campbell T, Puretzky A, Rouleau C, Geohegan DB, More K, Esker AR, Gibson HW, Dorn HC. Chem. Mater. 2010; 22(2): 347–351.
28. Ravindran S, Chaudhary S, Colburn B, Ozkan M, Ozkan CS. Nano Lett. 2003; 3(4):447–453.
29. Ravindran, S.; Chaudhary, S.; Ozkan, M.; Ozkan, CS. Biomicroelectromechanical Systems (Biomems). Vol. 773. 2003. Functionalization of carbon nanotubes for self assembly applications; p. 95-99.
30. Zou GZ. Chin. Chem. Lett. 2009; 20(3):356–357.
31. Alivisatos AP. Science. 1996; 271(5251):933–937.
32. Iezzi EB, Duchamp JC, Fletcher KR, Glass TE, Dorn HC. Nano Lett. 2002; 2(11):1187–1190.
33. Shultz MD, Duchamp JC, Wilson JD, Shu C-Y, Ge J, Zhang J, Gibson HW, Fillmore HL, Hirsch JI, Dorn HC, Fatouros PP. J. Am. Chem. Soc. 2010 Accepted.
34. Ge ZX, Duchamp JC, Cai T, Gibson HW, Dorn HC. J. Am. Chem. Soc. 2005; 127(46):16292–16298. [PubMed: 16287323]
35. Stevenson S, Rice G, Glass T, Harich K, Cromer F, Jordan MR, Craft J, Hadju E, Bible R, Olmstead MM, Maitra K, Fisher AJ, Balch AL, Dorn HC. Nature. 1999; 401(6748):55–57.
36. Peng HQ, Alemany LB, Margrave JL, Khabashesku VN. J. Am. Chem. Soc. 2003; 125(49):15174–15182. [PubMed: 14653752]
37. Shu CY, Corwin FD, Zhang JF, Chen ZJ, Reid JE, Sun MH, Xu W, Sim JH, Wang CR, Fatouros PP, Esker AR, Gibson HW, Dorn HC. Bioconjugate Chem. 2009; 20(6):1186–1193.

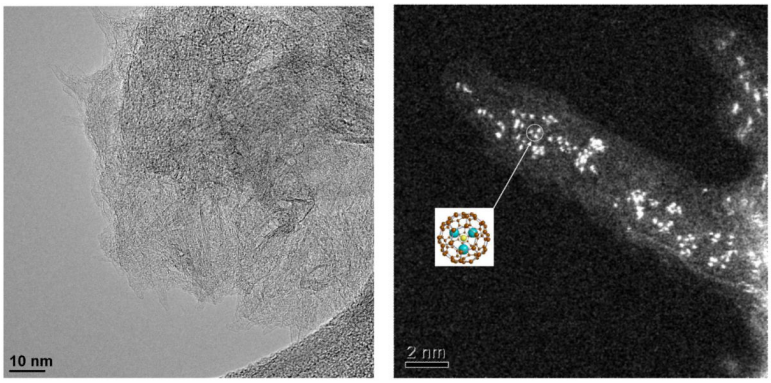

(a) (b)

Figure 1.

HRTEM image of $Lu_3N@C_{80}$@SWNHs (a) at low magnification and (b) high angle angular dark field image of $Lu_3N@C_{80}$@SWNHs at high magnification.

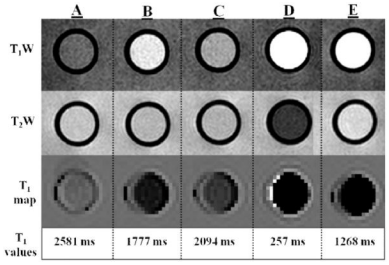

Figure 2.

(Top row): T_1-weighted images (T_R/T_E= 700 ms/10 ms). Second row: T_2-weighted images (T_R/T_E= 6000 ms/100 ms). Third row: T_1-map images (T_R/T_E= 1500 ms/29 ms). Bottom row: T_1 values of (A) functionalized SWNHs, (B) functionalized $Gd_3N@C_{80}$@SWNHs, (C) $Gd_3N@C_{80}$@SWNH-QDs, (D) $Gd_3N@C_{80}(OH)_{\sim 26}(CH_2CH_2COOM)_{\sim 16}$, (E) Omniscan. The concentrations of Gd^{3+} for (B)-(E) are 0.102 mM, 0.099 mM, 0.102 mM, and 0.102 mM respectively. The T_1 values are averages from regions of interest (ROI) within the tubes.

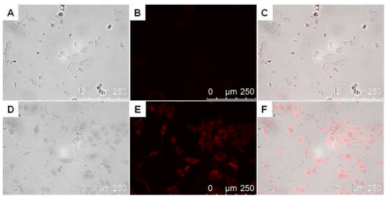

Figure 3.

Phase contrast images of RENCA cells (A) without $Gd_3N@C_{80}$@SWNH-QDs inclusion and (D) following 24 hours incubation with $Gd_3N@C_{80}$@SWNH-QDs. Fluorescence images of RENCA cells (B) without $Gd_3N@C_{80}$@SWNH-QDs inclusion and (B) following 24 hours incubation with $Gd_3N@C_{80}$@SWNH-QDs. Fluorescent images superimposed on phase contrast images of identical samples (C) without $Gd_3N@C_{80}$@SWNH-QDs inclusion and (F) following 24 hours incubation with $Gd_3N@C_{80}$@SWNH-QDs.

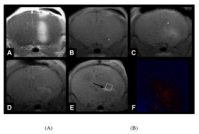

Figure 4.

(A) T_1-weighted MRI image enhanced with OMNISCAN™ (I.V.) revealing the tumor in the right hemisphere. (B) Baseline T_1W image prior to infusion of $Gd_3N@C_{80}$@SWNH-QDs into a U87 tumor bearing mouse brain. T_1W images (C) 3 hours (D) 1 day, and (E) 3 days post infusion showing bright contrast at the infusion site. (F) Post-mortem confocal laser scanning microscopy image of a region(indicated by the white box in E) from a 50 μm coronal vibratome section of the same mouse brainFollowing lambda scanning, spectral dye separation and removal of the signal due to autofluorescence, the signals that are retained match the spectral profiles of DAPI (blue) and quantum dots (red).

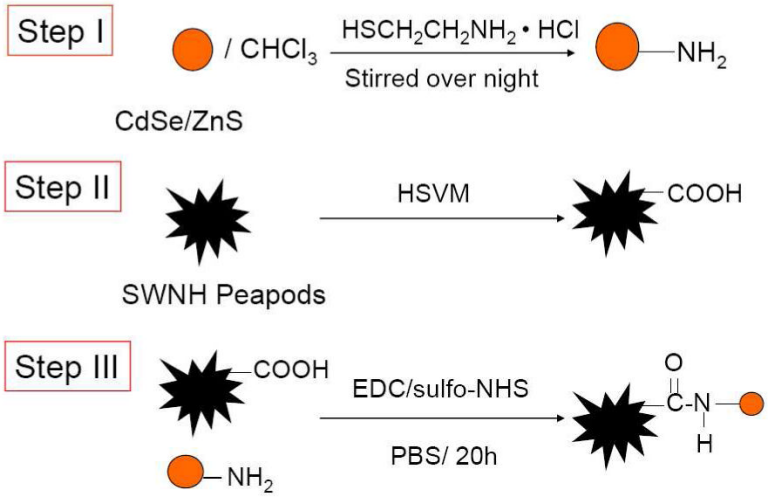

Scheme 1.

Depiction of conjugation of SWNHs with CdSe/ZnS QDs. The procedure contains three steps: I. Functionalization of QDs with AET; II. Functionalization of SWNHs peapods by HSVM method; III. Conjugation of SWNH peapods with QDs.